JPMTR 104 | 1804
DOI 10.14622/JPMTR-1804
UDC 655.1:777+532.56-035.67

Original scientific paper
Received: 2018-02-07
Accepted: 2018-03-30

# The impact of non-uniform ink absorption on flexographic print mottle

*Sofia Thorman[1,2], Li Yang[1], Anni Hagberg[1] and Göran Ström[1]*

[1] RISE Bioeconomy, Box 5604, 114 86 Stockholm, Sweden
[2] Karlstad University, Department of Engineering and Chemical Sciences, 651 88 Karlstad, Sweden

sofia.thorman@ri.se
li.yang@ri.se
anni.hagberg@ri.se
goran.strom@hotmail.com

## Abstract

Absorption non-uniformity and surface roughness of coated packaging boards are believed to have an impact on flexographic print mottle. Yet, their respective contributions are not well recognised due to their co-existence. Therefore, we propose a method that can solely study the effects of absorption non-uniformity on print mottle. This is achieved by artificially introducing uneven absorption, through well-controlled barrier patterns. The barrier patterns were added onto board surfaces using flexographic printing. By applying barrier patterns of several area coverages on board substrates of different intrinsic surface roughness it is possible to create a property-matrix, absorption non-uniformity versus for example surface roughness. With this matrix, the impact on print mottle from either of the properties can be studied independently. The results showed that surface roughness had a dominant effect on the print mottle, but mainly when comparing samples that spanned a broad roughness range. On the other hand, within a limited range of surface roughness, uneven ink absorption governed print mottle instead. This may explain why printing problems are sometimes encountered despite smooth board surfaces. Although the impact of absorption non-uniformity on print mottle differed from one board to another, the results indicated that a change towards more uneven absorption will have a negative impact on the print quality for most of the coated boards. The results give a better understanding of flexographic print quality and thereby can enable more reliable print mottle predictions.

**Keywords:** liquid packaging board, coated board, surface free energy, surface roughness, image analysis

## 1. Introduction and background

Liquid absorption and surface roughness are both possible sources of flexographic print mottle. However, their respective contribution and importance appear ambiguous in the literature. It can be difficult to separate their impact, using ordinary printed samples, since the two factors coexist and simultaneously may cause printing problems. Furthermore, there are several aspects of liquid absorption and all might not have the same relevance, and some are even difficult to characterise. Most of the measurement techniques capture only spontaneous (capillary driven) absorption on an average level while others capture forced absorption where an external pressure is applied and only a few techniques measure lateral uniformity. A significant number of scientific works show correlations between flexographic print quality and surface roughness of coated boards (Barros, Fahlcrantz and Johansson, 2005; Barros and Johansson, 2006; Jensen, 1989) and uncoated materials (Aspler, 2004; Lagerstedt and Kolseth, 1995; Wågberg and Wennerblom, 1992). The results are more diversified when it comes to liquid absorbency, and it has been suggested that absorbency has an impact on the print quality only under certain conditions. Sheng, Shen and Parker (2000) suggested that wettability (surface free energy) can have a dominating effect on ink transfer, but only when comparing samples of similar roughness. Aspler (2004), who did not find a correlation between print quality and liquid absorption, instead proposed that liquid absorption might cause problems when being extremely high or low, but has little effect when it lies within the "commercial norm". Lagerstedt and Kolseth (1995) suggested that one unfavourable property alone may not be that harmful, but a combination of two or more factors, e.g. a rough surface with unfavourable surface free energy, is more likely to cause problems.

As liquid absorbency can be linked to pore structure and surface free energy (Bosanquet, 1923; Lucas, 1918; Washburn, 1921), their impact on print quality have also been studied. For example, Lagerstedt and Kolseth (1995) saw a greater ink spreading and deeper ink penetration on coated samples of a more hydrophilic nature, Olsson, et al. (2006) reported that the polarity of coated samples has positive impact on solid tone print density, and Bassemir and Krishnan (1991) suggested that a high polarity can improve the print uniformity. There are reports of deeper ink penetration on more porous coatings, whereas more closed structures improved ink holdout and increased ink spreading (Bohlin, 2013; Preston, et al., 2008). It has also been suggested that ink solids are retained on the coating surface when having a high adsorptive surface area in combination with a low permeability, meaning that the wetting front spends longer time on the surface (Ridgway and Gane, 2002).

Nevertheless, we occasionally come across samples where a print quality issue cannot be explained by either surface roughness or by the average absorption rate. In these cases, absorption non-uniformity may be a possible source of the problem. To our knowledge, little has been published regarding the impact of non-uniform absorption on flexographic print quality. But, as pointed out by Preston, et al. (2008), a uniform ink spreading can be of crucial importance to avoid flexographic print mottle.

The relative importance of uneven absorption, when compared to surface roughness, has seldom been studied systematically. There are two major reasons, (a) it is difficult to obtain samples, between which only their absorption uniformity differs and (b) there has been a lack of relevant measuring techniques when it comes to the evenness of short-time absorption of aqueous liquids (inks). The objective of this study was to gain a better understanding of how board properties impact flexographic print mottle and specifically to decuple the impact of uneven ink absorption from that of surface roughness. We focus on non-uniform capillary driven absorption and propose a method to separately study its effect on flexographic print mottle.

## 2. Methods and materials

This section describes how absorption non-uniformity can be modified by adding a barrier in form of halftone patterns onto coated board surfaces. When the dot percentages of the halftone barrier patterns vary, various levels of absorption non-uniformity can be created without impacting on other properties of the samples. By doing this on a set of coated board samples, the impact from uneven ink absorption can be studied on boards of e.g. different surface roughness. The patterns were examined in several ways to ensure that only the absorbency and surface chemistry were modified, without the surface roughness being considerably affected. The impact on print mottle by the patterns was then studied. Creation of barrier patterns, printing and testing of contact angle and absorption non-uniformity were made in a laboratory with well-controlled climate conditions: temperature 23 °C ± 1 °C and relative humidity (RH) 50 % ± 2 %.

### 2.1 Board materials

Seven paper boards were used in this study: four pilot-coated boards (denominated P1, P2, P3, and P4) and three commercially produced boards (denominated CA, CB, and CC). Together, they covered a broad range of surface roughness and surface chemistry, see Table 1.

The pilot-coated boards featured the same 200 g/m$^2$ duplex base board (Klabin S.A., Brazil) and the same pre-coating (100 pph Hydrocarb® 60 and 13 pph latex type A) but had different top coating formulations, see Table 2. Combinations of four ground calcium carbonate (GCC) pigments (Omya International AG, Oftringen, Switzerland), two types of lattices, thickener (FinnFix 10, Noviant Oy, Finland) and caustic soda (NaOH) were used in the pre-coating (11.8–12.5 g/m$^2$) and top-coating (11.3–12.0 g/m$^2$) formulations. A vinyl acetate acrylate latex (CHP 2635EP, CH Polymers Oy, Raisio, Finland) with $T_g$ = 15 °C is referred to as latex type A and a styrene butyl acrylate (Acronal S722, BASF, Ludwigshafen, Germany) with $T_g$ = 23 °C is referred to as latex type B. Increasing the latex content (type A) in the top coating created a more closed structure, while the second latex (type B) created a more hydrophobic coating. The Hydrocarb® 90 (90 % of its particles < 2 μm) and Setacarb® HG (98 % < 2 μm) carbonates have a broad particle size distribution (PSD), whereas Covercarb® 75 (75 % < 1 μm and 95 % < 2 μm) has a narrow PSD. The coating pigment with a narrow PSD gave a greater pore volume and pore size than the broad PSD pigment and the more latex in the coating colour the lower the porosity. Hence, sample P4 had the highest porosity, samples P2 and P3 had the lowest porosity and sample P1 was in-between. The pilot coating was made at 600 m/min with a Jagenberg bent ceramic blade (angle approx. 18°).

Two of the commercial products were coated liquid boards for flexographic printing, referred to as CA and CB (supplied by BillerudKorsnäs, Sweden, and Tetra Pak, Sweden, in no particular order). As a reference, a cast-coated offset grade Chromolux 700 (Zanders GmbH, Germany), of high smoothness, was included and is referred to as CC. Elemental identification using scanning electron microscopy (SEM), SU3500 (Hitachi High-Technologies Europe GmbH, Krefeld, Germany),

*Table 1: Surface roughness (standard deviation of height about the mean, lateral wavelength interval of 0.06–1 mm) and contact angle with water (after 0.1 s); ± 95 % confidence interval*

| Paper board properties | 15 Latex A P1 | 20 Latex A P2 | 20 Latex B P3 | N75 GCC P4 | Com. A CA | Com. B CB | Com. C CC |
|---|---|---|---|---|---|---|---|
| Roughness [µm] | 0.86 ± 0.03 | 0.75 ± 0.02 | 0.76 ± 0.01 | 0.86 ± 0.01 | 1.13 ± 0.04 | 0.82 ± 0.04 | 0.28 ± 0.01 |
| Contact angle [°] | 78.3 ± 1.1 | 77.3 ± 0.5 | 85.8 ± 0.6 | 75.4 ± 0.5 | 83.1 ± 0.6 | 82.6 ± 1.1 | 86.4 ± 1.2 |

*Table 2: Coating formulations of the four pilot-coated boards (all with the same pre-coating); 0.5 pph thickener and 0.08 pph caustic soda were used in all compositions*

| Sample code | Latex [pph] | | GCC pigment [pph] | | |
|---|---|---|---|---|---|
| | Type A | Type B | Hydrocarb 90 | Setacarb HG | Covercarb 75 |
| P1 | 15 | | 60 | 40 | |
| P2 | 20 | | 60 | 40 | |
| P3 | | 20 | 60 | 40 | |
| P4 | 15 | | | | 100 |

with energy dispersive x-ray analysis indicated that all three commercial boards contained clay and calcium carbonate in the top-coating layer. Clay content was higher than calcium carbonate content and the composition was similar for all three samples.

### 2.2 Creation of absorption non-uniformity with barrier patterns

Absorption non-uniformity was introduced to the board surfaces by adding a barrier in a halftone pattern. Barrier dots may fill the pore structure and/or modify the surface chemistry, both of which alter the ink absorption locally. Nine barrier tones were included (ranging from 2 % to 14 %) and the board itself (0 %), and the higher the tone value, the more uneven the absorption became. Impact on print mottle was a function of the actual absorption pattern that had been created, and not a direct function of the nominal-tone value.

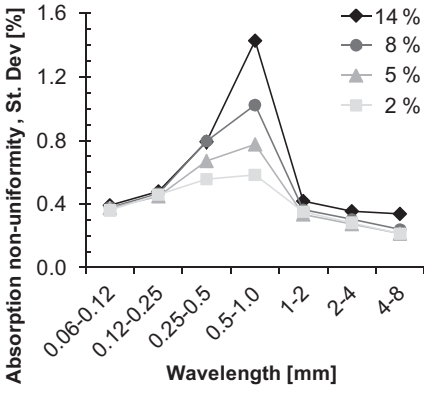


*Figure 1: Example of barrier patterns, on sample P1, causing non-uniform absorption with a peak around lateral wavelengths of 0.5–1 mm; the non-uniformity increased with the nominal tone*

A coarse screen ruling was used, 31 lpi, which means that the barrier patterns primarily created non-uniformity in the lateral wavelength interval of 0.25–8 mm, peaking at 0.5–1 mm. The absorption non-uniformity for some barrier tones is shown in Figure 1. The procedure to characterise the absorption non-uniformity is explained in the section 2.5 Characterisation of spontaneous absorption non-uniformity.

The patterns were created through flexographic printing with a F1 Printability tester (IGT Testing Systems, Amsterdam, Netherlands) and using the vehicle of a flexographic ink (including binder, additives and solvent, but excluding colorant). The ink was a Siegwerk ink designed for printing at Tetra Pak, Lund, Sweden. Following press-settings were used: anilox with volume of 2.7 $cm^3/m^2$ (IGT Testing Systems, Amsterdam, Netherlands), UVR 1.7 mm printing plate (MacDermid Printing Solutions Europe, France, with 70 Shore A durometer hardness), speed of 0.5 m/s and the pressure set to 25 N in both the printing and anilox nip. The printing plate was inked once and then directly brought into contact with the board substrate. The barrier printed samples were left to dry for at least three days in a climate-controlled room at 23 °C and an RH at 50 %, nominally.

### 2.3 Characterisation of surface porosity

The barrier patterns are expected to change the pore structure locally and to reduce the surface porosity by blocking the surface pores either fully or partly. This was verified by examining the two extreme samples, namely commercial sample CC that had a very low surface porosity and, the pilot-coated sample P4 that had quite open surface pore structure. The SEM images were taken after the sputtering of a conductive mono-

layer with a gold/palladium (Au/Pd) alloy. The secondary electron emission from the surface of the samples was detected in a Jeol 6 700 field emission SEM (JEOL Ltd., Tokyo, Japan), using a primary electron beam of 5.0 kV to bombard the samples.

In addition to the SEM imaging technique, maps of surface porosities were acquired using measurements of local refractive indices over an area of 50 mm × 50 mm, using a Surfoptic Imaging Reflectometry System (Data Systems Ltd., Bristol, United Kingdom). This measurement detects refractive index (RI) in the top surface, at less than 1 µm depth (Hiorns, Kent and Parsons, 2005). The porosity map is displayed as a greyscale colour map, where a greater RI is represented by brighter pixels.

Coating pigments, the binder, as well as the ink vehicle, were expected to have rather similar refractive indices (around 1.5–1.6), whereas air (1.0) differed significantly. This means that the larger the porosity (air-content) in the surface layer, the lower the RI and the darker the grey-scale image areas will be.

### 2.4 Characterisation of contact angle and surface free energy

The total surface free energy, polar and apolar parameters were calculated from contact angle measurements, using the Owens and Wendt method (Owens and Wendt, 1969). This was made for the original board surfaces without any barrier and for solid tones of the barrier on each of the boards.

The contact angles were measured with a dynamic contact angle tester (DAT from FIBRO system AB, Hägersten, Sweden). The contact angle readings were taken at 0.1 s for deionised water (treated by reverse osmosis and deionisation at RISE Bioeconomy, Stockholm, Sweden) and at 0.8 s for diiodomethane (for synthesis, Merck KGaA, Schuchardt, Germany). The drops had stabilised, and the liquid volumes were quite steady around these times. The average contact angle of eight drops is given, within the ± 95 % confidence interval.

### 2.5 Characterisation of spontaneous absorption non-uniformity

Absorption non-uniformity was characterised with a staining technique, using an aqueous liquid consisting of deionised water, 0.025 % of methylene blue dye (C.I. 52015, Merck KGaA, Darmstadt, Germany) and 0.07 % mass fraction of Surfynol 2502 (acquired from Air Products Chemicals Europe BV, now marketed by Evonik Industries AG, Essen, Germany). The latter is a surfactant that reduces the surface tension of the coloured liquid and is normally used in flexographic inks. The coloured liquid was first applied on the sample and, after tenths of a second, the excess liquid was removed with blotting paper. A modified F1 Printability tester (IGT Testing Systems, Amsterdam, Netherlands) was used to transport the sample from the specially made liquid applicator (a container that is open at the bottom and placed on the sample) to the nip where a blotting paper removes the excess liquid and leaves a stain on the sample (Thorman, et al., 2012). A laterally uneven stain is related to absorption non-uniformity and white-top mottle. Their respective contributions are separated in the analysis using the red (R) and blue (B) image channels, as described by Thorman, Yang and Hagberg (2013).

### 2.6 Image capturing and analysis

The absorption stains and flexographic prints were scanned in RGB with a flatbed scanner, Epson Perfection V750 Pro (Seiko Epson Corp., Japan), using a gamma value of 1.2 and a resolution of 1200 dpi. These images were analysed with STFI Mottling software (RISE Bioeconomy, Stockholm, Sweden). A calibration set was included in each scan, enabling calibration of each image channel to reflectance. The images of the printed samples were converted to grey-scale before assessing the variations, whereas the absorption non-uniformity was assessed, based on the re-constructed R-channel image:

$$R_{\text{absorption}} = \frac{R_{\text{red}}}{R_{\text{blue}}} \times \bar{R}_{\text{blue}} \qquad [1]$$

where $R_{\text{red}}$ and $R_{\text{blue}}$ are the reflectance values of the individual pixels in the R and B channels respectively, and $\bar{R}_{\text{blue}}$ the average reflectance in the B-channel image (Thorman, Yang and Hagberg, 2013).

Absorption non-uniformity or print mottle was calculated as the standard deviation of the reflectance values for the pixels within a 21 mm × 21 mm area. Through a Fast Fourier Transform (FFT), the absorption or the print heterogeneity of each image area was divided into spatial wavelength intervals. Standard deviation in the wavelength interval of 0.5 mm to 8 mm is reported. Two areas per sample and barrier tone were analysed, each being 21 mm × 21 mm.

### 2.7 Characterisation of surface roughness and topography of barrier patterns

The surface roughness of the boards (without barrier) was characterised as height variations about the mean (standard deviation) in the spatial wavelength interval of 0.25 mm to 1 mm. Eight areas of 13 mm × 13 mm were analysed per sample, with a lateral resolution of 12.7 µm. The measurements were made using the photometric stereo technique on an OptiTopo instrument (RISE Bioeconomy, Stockholm, Sweden).

To characterise the topography of the transparent barriers accurately, replicas of the surfaces were cast with a fast-curing two-part silicon rubber compound (RepliSet-GF1 from Struers A/S, Ballerup, Denmark) and measured with the OptiTopo instrument (image area of 15.6 mm × 15.6 mm, resolution of 16.0 µm). One replica (measurement) was made from the coating layer and one with a 10 % barrier tone on each board. Consequently, the roughness was not expected to be exactly the same, due to variations within the sample.

### 2.8 Printing and print quality evaluation

A solid cyan was printed on the patterned surfaces to evaluate the impact resulting from non-uniform absorption. The laboratory flexographic press, anilox, plate type and speed were the same as when applying the barrier patterns, whereas the pressure was set to 100 N in the printing nip and 75 N in the anilox nip. The complete Siegwerk ink was used, including colorant, which had a surface tension and viscosity of 38.6 mN/m ± 0.1 mN/m (at 300 s with Wilhelmy plate method) and 19 s efflux time (DIN cup 4 mm, temperature 23 °C ± 1 °C), respectively.

To compensate for an uneven inking along the printing direction in the F1 Printability tester, the printing plate was inked for two revolutions before being brought into contact with the patterned board surfaces and two strips were printed in opposite directions. That is, one strip goes from 0 % to 14 % of the barrier patterns and another one in the reversed direction by turning the patterned surface by 180 degrees. The mottle of the solid cyan print is the average of these two stripes. For a couple of strips, a few of the tone values had to be left out, because of defects in the inking. Print mottle was used as a measure of the heterogeneity of the solid cyan prints and was calculated as the standard deviation of reflectance values within full-tone printed areas (each pixel having an individual reflectance value). The printed samples were scanned and print mottle analysed as set out in section 2.6 Image capturing and analysis.

### 2.9 Linear regression analysis

Statistical analysis of relation between the dependent variable (print mottle, $y$) and independent variable (absorption non-uniformity, $x$) was made in the opensource software R (R Foundation for Statistical Computing, Vienna, Austria). The $y$ was regressed onto $x$ to create a model for each sample (James, et al., 2013):

$$\hat{y} = \hat{\beta}_0 + \hat{\beta}_1 x \quad [2]$$

where the coefficient $\hat{\beta}_0$ represents an estimate of the intercept of the model with $y$-axis and $\hat{\beta}_1$ represents an estimate of the slope of the model. The $\hat{y}$ indicates a prediction of print mottle based on absorption non-uniformity measurement. Estimates of the coefficients were produced so that the linear model fitted available data and the residual sum of squared errors (*RSS*) was minimised,

$$RSS = \sum_{i=1}^{n} \left(y_i - \hat{\beta}_0 - \hat{\beta}_1 x_i\right)^2 = \sum_{i=1}^{n} (y_i - \hat{y}_i)^2 \quad [3]$$

and to minimise *RSS,* following equations were used:

$$\hat{\beta}_1 = \frac{\sum_{i=1}^{n}(x_i - \bar{x})(y_i - \bar{y})}{\sum_{i=1}^{n}(x_i - \bar{x})^2} \quad [4]$$

$$\hat{\beta}_0 = \bar{y} - \hat{\beta}_1 \bar{x} \quad [5]$$

where $n$ is the number of data points, $y_i$ and $x_i$ the measurement data of print mottle and absorption non-uniformity related to the $i$-th data point, respectively, $\hat{y}_i$ the predicted print mottle value from the model, and the averages of the measured $x$- and $y$-values are represented by $\bar{x}$ and $\bar{y}$, respectively.

The accuracy of the models and their coefficients was assessed by $R^2$ statistics that quantify how well each model fits the data. The accuracy of the coefficient estimation was assessed by their standard error and $p$-value. The $p$-value indicates the probability of observing this relation between $x$ and $y$ due to random chance. Detailed description of how the $R^2$ statistics, $p$-values and standard errors are calculated can be found elsewhere, e.g. James, et al. (2013).

## 3. Results

In this section, we first present the results of print quality and how this has been affected by surface roughness and uneven absorbency. This is followed by characterisations of the barrier patterns.

### 3.1 Print mottle on the untreated board samples

A linear correlation ($R^2$ = 0.69) was observed between the print mottle and the surface roughness, for the boards without barrier patterns (Figure 2a). However, this is largely due to the commercial samples which considerably extended the roughness range. However, the correlation become less obvious for the pilot-coated boards, which were in the mid-roughness range (0.6–0.7 µm). On the contrary, no general correlation between the non-uniform absorption and the print mottle was found (Figure 2b) when considering both the commercial and the pilot-coated boards. Nevertheless, within the group of the four pilot-coated boards, the correlation was very high ($R^2$ = 0.98). These two graphs reveal that a correlation between

print mottle and surface roughness does not rule out that the print may simultaneously be affected by uneven ink absorption, but possibly to a lesser extent.

### 3.2 Property matrix

We introduced well-controlled barrier patterns to manipulate the absorption non-uniformity of the coating surfaces. By applying these barrier patterns of several area coverages on board substrates having different intrinsic surface roughness, we received a property matrix, as illustrated in Figure 3. Since the board samples may differ in more aspects than surface roughness, the *x*-axis may also include some other property than surface roughness, or the combined effect of several properties of the boards.

The matrix can be utilised to isolate the impact of absorption non-uniformity from that of surface roughness, or vice versa. This can be done by comparing samples having the same property value in one axis but having different values in the other axis, as illustrated by the dashed rectangles. Within the horizontal rectangle, the samples are compared at the same level of absorption non-uniformity, meaning that print mottle is interpolated/extrapolated to a given absorption level and then compared with e.g. surface roughness. Within the vertical rectangle, the comparison is made between print quality that was obtained with the different barrier patterns (i.e. absorption non-uniformities) on one board. By using the property matrix, it was possible to study if uneven absorption had an impact on print mottle only on pilot-coated boards in the mid-roughness range or if it also would affect the print on the rougher and smoother commercial boards.

#### 3.2.1 The importance of absorption non-uniformity at constant roughness

The impact on print mottle from changes in absorption uniformity was studied with the barrier patterns on the individual board samples. As the tone-value of the barrier pattern increased, the absorption became more uneven and, in turn, this had a negative impact on the print quality. The cyan print on the barrier dots was brighter than on the untreated coating layers, an example from sample P4 is shown in Figure 4. In most of the cases, there was a strong linear correlation between the print mottle and the absorption non-uniformity (see Figure 5). This was also true for the commercial

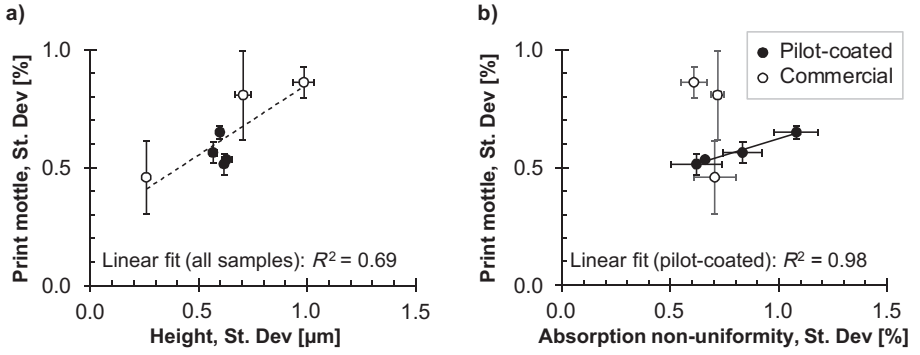


*Figure 2: Print mottle plotted versus: a) surface roughness and b) absorption non-uniformity; where regression line in graph a) has been calculated from pilot-coated and commercial boards as one series; the error bars indicate a 95 % confidence interval*

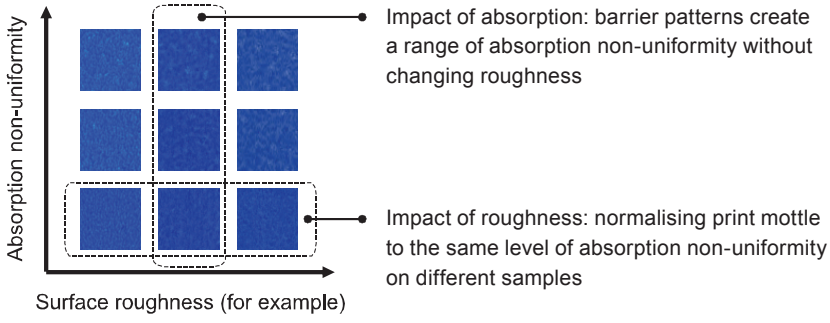


*Figure 3: Illustration of property matrix and how it can be utilised when separating the impacts on print mottle resulting from absorption non-uniformity and from, for example, surface roughness*

boards, even though Figure 2a indicated that print mottle ranking among these boards was pre-dominantly controlled by surface roughness.

When uneven absorption was introduced, the impact on print mottle was significant on certain samples but modest on others. The steeper the gradient of the regression line, the more sensitive print mottle was to uneven absorption. For example, there was a linear 1:1 correlation between the print mottle and the absorption non-uniformity for sample P4, whereas the gradient was not as steep for samples P1 and P2 (Figure 5a and Table 3). The effect on print mottle was modest when absorption became uneven on sample CB but possibly the impact increased at higher level of absorption non-uniformity (Figure 5b). Table 3 shows that absorption non-uniformity testing was able to explain a large part of the variability in print mottle on each of the five samples. The high $R^2$-values, ranging from 0.74 to 0.98, indicated that the linear models fitted the data well. The $p$-values for the absorption non-uniformity coefficients were small (in four cases < 0.001 and in one case < 0.01), which indicated that it is unlikely to observe such substantial association between predictor and response due to random chance. Hence, we conclude that a real association between absorption non-uniformity and print mottle exists.

The barrier patterns successfully altered the absorption non-uniformity on five of the samples without creating a topographical pattern with raised (elevated) dots and on these samples the capillary driven absorption test detected the patterns as expected. Results from these boards are shown in Figure 5. Two samples, commercial sample CC and pilot-coated sample P3, were omitted due to a topographical effect and/or the absorption test not being able to correctly detect the absorption non-uniformity, see results in section 3.3 Characteristics of the barrier patterns.

#### 3.2.2 The importance of surface roughness at constant absorption non-uniformity

The regression analyses of individual boards (Table 3) were utilised to make predictions (interpolations/extrapolations) of print mottle values corresponding to two separate levels of absorption non-uniformity. In Figure 6, the print mottle values have been estima-

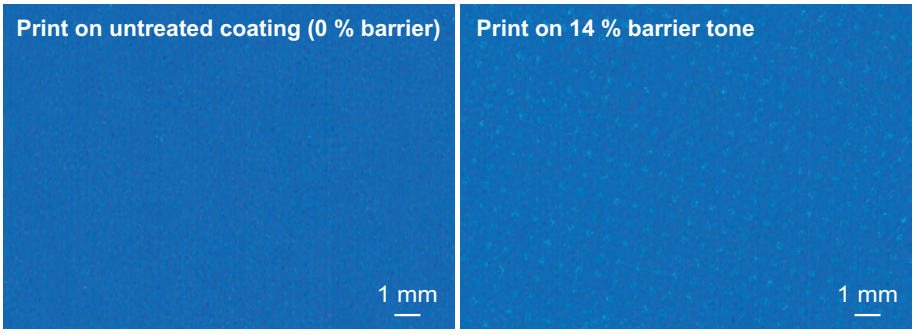


*Figure 4: Solid cyan printed on the untreated (left) and absorption modified (right) board surfaces of sample P4; the brightness of the images has been enhanced for better visualisation*

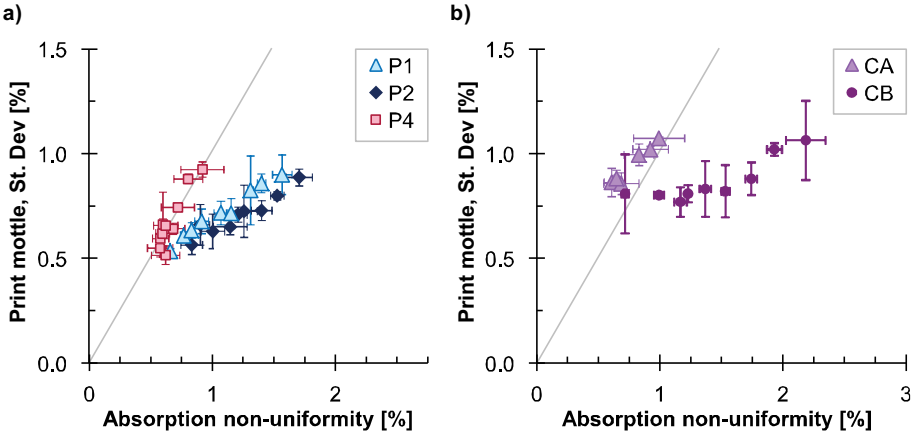


*Figure 5: Print mottle versus absorption non-uniformity of the paper boards with barrier tones ranging from 0 % to 14 %; the error bars indicate a 95 % confidence interval*

*Table 3: Linear regression analyses of print mottle regressed onto absorption non-uniformity (data from Figure 5), where coefficients for intercept ($\hat{\beta}_0$) and gradient ($\hat{\beta}_1$) and their respective standard errors are given; the p-values are indicated by stars, the $R^2$ quantifies accuracy of the models*

| | P1 | P2 | P4 | CA | CB |
|---|---|---|---|---|---|
| $\hat{\beta}_1$ (absorption non-uniformity) | 0.39 *** | 0.32 *** | 1.09 *** | 0.57 *** | 0.19 ** |
| Standard error ($\hat{\beta}_1$) | 0.02 | 0.04 | 0.16 | 0.06 | 0.04 |
| $\hat{\beta}_0$ (intercept) | 0.30 *** | 0.32 *** | −0.05 | 0.50 *** | 0.59 *** |
| Standard error ($\hat{\beta}_0$) | 0.03 | 0.05 | 0.11 | 0.05 | 0.06 |
| $n$ | 8 | 8 | 9 | 5 | 8 |
| $R^2$ | 0.98 | 0.91 | 0.85 | 0.95 | 0.74 |

*** $p$-value < 0.001; ** $p$-value < 0.01; * $p$-value < 0.05

ted for absorption non-uniformity of 0.5 % and 1.0 %, respectively. It is evident that surface roughness had greater impact on print mottle when absorption non-uniformity was lower and on a constant level. We do not consider it applicable to extrapolate down to a perfectly uniform absorption state, since the barrier patterns only have added rather than diminished the unevenness. Therefore, we suggest only making forecasts of print mottle at absorption non-uniformity levels that are equal or higher than 0.5 %.

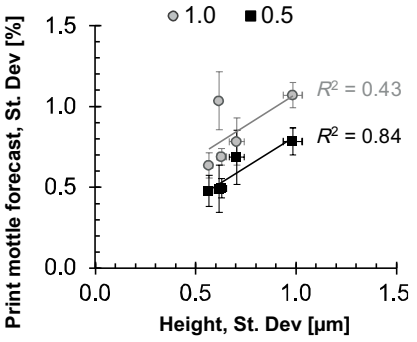


*Figure 6: Predictions of print mottle at two absorption non-uniformity levels (1.0 % and 0.5 %) versus surface roughness; the error bars indicate 95 % confidence interval (prediction interval for y-axis)*

### 3.3 Characteristics of the barrier patterns

#### 3.3.1 Topography of the barrier patterns

Any topographical pattern resulting from the barrier dots, was expected to be seen in the height spectra, as surface roughness and as surface peaks. The surface roughness measurements of the replicas indicated that the barrier dots may have created topographical modifications on three samples, i.e. P3, CB and CC, see Figure 7a. This observation is probably true for commercial sample CC, but it is unlikely to apply to the other two samples. Sample CC had a very smooth coating surface, where 93 % of the barrier dots were higher than the rest of the sample, but only by 0.1 µm. More precisely, the barrier dots were about 0.7 µm above the average height (the zero level), and the board in-between the barrier dots was often as high as 0.6 µm and never raised above the barrier dots. The height spectra of this sample also indicated a periodic pattern, which likely was connected to the barrier dots, see Figure 7b.

On the contrary, the original surfaces of the other two boards were much rougher, and only a few of the barrier dots raised above the rest of the board surface. Hence, the evidence that the barrier patterns altered their topography was not strong for sample P3 or CB. As a matter of fact, only 9 % to 10 % of the dots were raised above the other surface areas while as much as 83 % and 72 % of the surface peaks, respectively, were not connected to barrier dots. Our conclusion is that the barrier patterns did not change the topography on six of the seven samples.

### 3.4 Surface porosity

Figures 8 and 9 show the SEM images of sample P4 and sample CC whose surfaces contained the most open and the most closed coating structures. As shown, the barrier dots have partly filled and/or blocked the surface pores on both surfaces. The images also reveal that the coverage was not uniform within the dots and the porous structures of the coating layers were covered in some parts but remained more open in other parts of the dots. Even when the barrier material covered the porous structure of the coating layer, micro-pores appeared to be present in the barrier material.

Surface porosity measurements, based on RI, gave similar indications as the SEM images. In Figure 10, a periodic pattern is clearly visible in the porosity map for sample P4. More porous areas possess more air and have lower RI (around 1.0). The coating pigment, binders and ink vehicle were not expected to be easily distinguished from one another, due to their similar refractive indices (around 1.5–1.6). Hence, sample P4 displayed a sharp contrast between the porous coating and closed barrier dots. On the contrary, the pattern

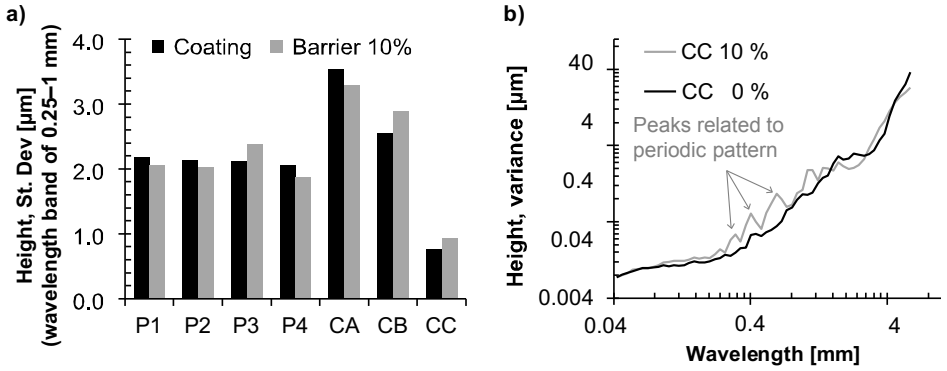


*Figure 7: Surface roughness measured on one replica of each coating layer and 10 % barrier pattern on each sample (a); height spectra of board CC (b) before and after adding a barrier pattern*

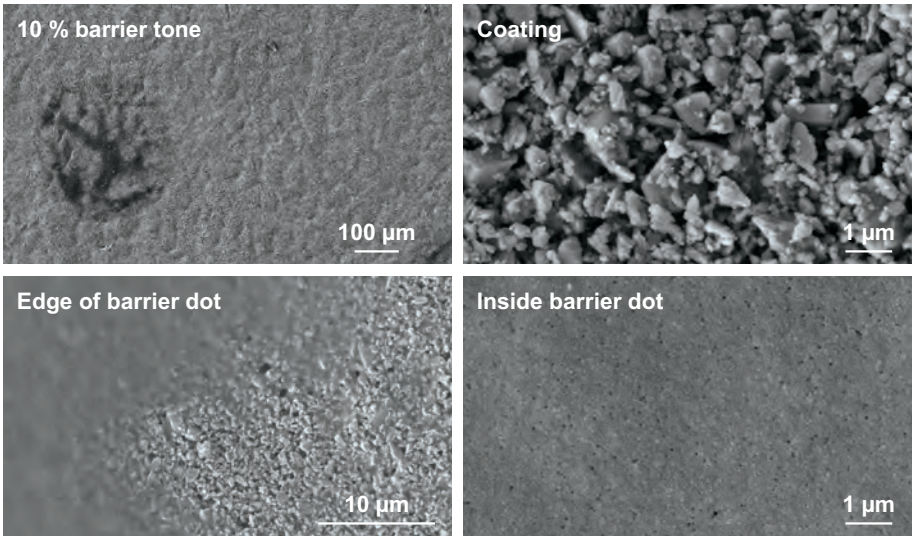


*Figure 8: The SEM images of the coating and barrier dots on pilot-coated sample P4; this coating has a very open structure due to broad particle-size distribution of the calcium carbonate pigments*

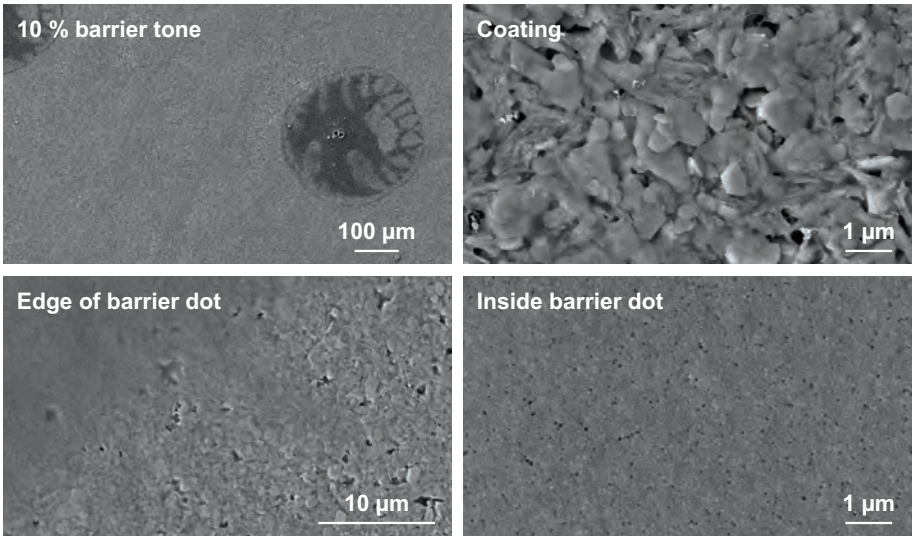


*Figure 9: The SEM images of the coating and barrier dots on commercial sample CC; this coating has a very closed structure*

was hardly visible in the surface porosity map of sample CC due to a much more closed coating structure.

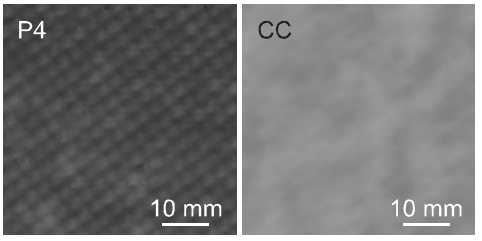


*Figure 10: Surface porosity maps of 10 % barrier tones on the open coating of P4 and the closed coating of sample C; darker pixels correspond to lower refractive index, i.e. surface pores are dark*

### 3.5 Absorbency and surface chemistry

The barrier patterns caused an uneven absorption due to closed surface pores and/or a modified surface chemistry. The patterns were most often observed as brighter dots in the stains made by the coloured water, see Figure 11. All the barrier dots received a certain amount of the stain, but the absorbency of the board itself made a stronger impact and created a contrast between low absorbing barrier dots and "high" absorbing board. Samples CC and P3 displayed rather low absorption levels due to low porosity and/or low hydrophilicity, which caused those coatings to be either equally stained or even brighter stained than the barrier dots.

In general, the absorption non-uniformity increased with the barrier tone value, as is shown in Figure 12, even though the impact from the barrier patterns differed among the samples.

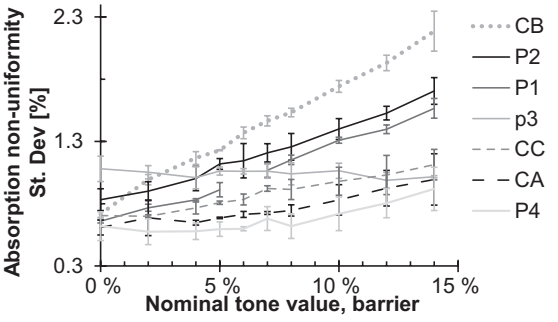


*Figure 12: Absorption non-uniformity was created by the barrier patterns on the board samples; the error bars indicate the 95 % confidence interval*

As already seen, the barrier material partly filled in (or closed) the surface pores (see Figures 8 and 9), but it also changed the surface chemistry. In most cases, water wetted the barrier material more easily than the board surfaces, due to a higher surface energy and a more polar nature of the barrier material, see Figure 13.

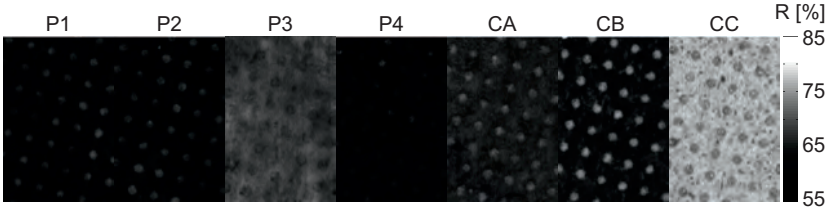


*Figure 11: Absorption patterns (14 % nominal tone) in the stains from the coloured water; images show the reconstructed R-channel images (Equation 1), each area is 3.6 mm × 5.4 mm*

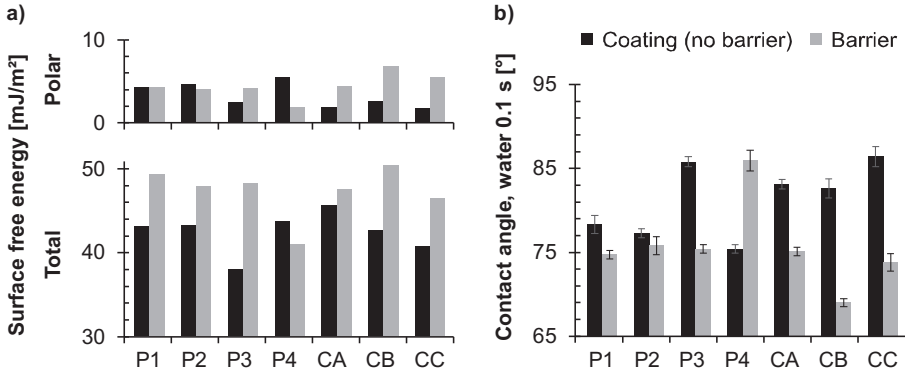


*Figure 13: Characterisation of the coating layers and their counterparts covered by a solid barrier tone; a) the total surface free energy (bottom) and the polar component of the surface free energy (top), and b) contact angle of water droplets, a 95 % confidence interval is indicated in b)*

With a surface tension of 38.6 mN/m, the printing ink can be expected to wet all the board and barrier surfaces.

## 4. Discussion

For five of the samples, the untreated board surfaces absorbed more coloured water and acquired a stain that was darker than on the barrier dots. This is attributed to the fact that the barrier material had closed many of the surface pores and, thereby, hindered absorption (Figures 8 to 10). Nevertheless, the barrier dots still acquired a slight bluish shade from the stain. This may be a consequence of the barriers having a favourable surface chemistry with higher surface energy (Figure 13), thus causing them to be wetted easily and, thereby, making it possible for adsorption/deposition of the cationic methylene blue dye to occur.

There were two exceptions where the coatings did not become darker than the barrier dots in the absorption stains (Figure 11). On sample P3, the stain appeared as equally bright on the coating layer as on the barrier dots. This could be explained as a combined effect of low absorbency of the untreated board surface, due to its hydrophobicity that originates from the latex (type B) used in the coating, while the barrier dots were wetted more easily due to higher surface free energy. A similar effect was observed on sample CC, where the stain was even brighter on the board surface than on the barrier dots. Manual tests indicated that also stains on coatings P3 and CC would become darker than on the barrier dots after longer absorption time. This suggests that the colorant in the absorption test was adsorbed on the barrier dots and that the absorption by the coating outside the barrier dots was slow on these particular samples. Since untreated sample CC gave the lowest print mottle, the findings also suggest that strong absorption is not necessary for high print quality as long as it is even.

Unlike the results from the absorption test, all the barrier dots were observed to be brighter on the printed samples, including samples P3 and CC. We suggest that this is primarily due to reduced accessibility to the surface pores rather than modification of the surface chemistry. The effects of the surface chemistry which caused the absorption/wetting to be slow on samples P3 and CC, will be subdued by the nip pressure when printed in the laboratory press. This suggests that the uneven pore structure was most probably responsible for the print mottle that increased with the tone-value of the barrier pattern. When it came to the extreme samples whose original surfaces had very low absorbencies in combination with the easily wetted barrier dots, absorption non-uniformity may not be accurately predicted when using the spontaneous absorption test.

## 5. Conclusions

Adding a barrier pattern, to control the level of absorption non-uniformity, has proven to be a powerful tool. With this approach, it is possible to study the impact of absorption separately and to compare the impact of surface roughness, for example, when absorption is maintained at a constant level.

With this study, we have gained a better understanding for how and when absorption non-uniformity and surface roughness are of importance. Absorption non-uniformity indeed contributed to print mottle both on rough and smooth boards, but it did not have equally strong impact on all samples. It appears that a change towards a more uniform absorption will have a larger impact on certain boards. The reason for this needs to be investigated further. Secondly, surface roughness accounted for a large part of the print mottle and when comparing two boards of large roughness difference the smoother surface is likely to have less print mottle.

Absorption non-uniformity may result from non-uniformity either in pore structure or surface chemistry, where the pore structure appeared to have a greater impact on print mottle. Finally, for surfaces with a slow absorbency/wetting, spontaneous absorption non-uniformity tests need to be accompanied by characterisations of forced absorption.

**Acknowledgements**

The authors wish to thank the industrial partners, BillerudKorsnäs, Stora Enso, Tetra Pak, ITC, Klabin, Metsä Board, Metsä Fibre, and WestRock for financing and supporting this research. This study was performed within the Industrial Graduate School VIPP (Values Created in Fiber Based Processes and Products) with financial support from the Knowledge Foundation, Sweden. The study was partly funded with strategic competence funds from RISE, Sweden. Last but not least, we would gratefully like to thank Mr Martin Taylor and Miss Eli Gaskin at Imerys for characterising surface porosity and making SEM images.

## References


Aspler, J., 2004. Print quality test methods for linerboard. In: *2004 TAGA Proceedings: 56th Annual Technical Conference*. San Antonio, USA, 18–21 April 2004. Sewickley: Technical Association of the Graphic Arts, pp. 428–452.

Barros, G.G., Fahlcrantz, C.M. and Johansson, P.Å., 2005. Topographic distribution of uncovered areas (UCA) in full tone flexographic prints. *TAGA Journal*, 2(1), pp. 43–57.

Barros, G.G. and Johansson, P.Å., 2006. Prediction of uncovered area occurrence in flexography based on topography: a feasibility study. *Nordic Pulp & Paper Research Journal*, 21(2), pp. 172–179.

Bassemir, R.W. and Krishnan, R., 1991. Surface and colloidal aspects of dynamic ink/paper interactions during printing. In: *Proceedings of CPPA/TAPPI Symposium on Papercoating Fundamentals*, Montreal, Canada, 17–18 May 1991. Montreal: Canadian Pulp and Paper Association, pp. 69–75.

Bohlin, E., 2013. *Surface and Porous Structure of Pigment Coatings: Interactions with Flexographic Ink and Effects on Print Quality.* PhD Thesis. Karlstad University.

Bosanquet, C.H., 1923. On the flow of liquids into capillary tubes. *The London, Edinburgh, and Dublin Philosophical Magazine and Journal of Science: Series 6*, 45(267), pp. 525–531.

Hiorns, A.G., Kent, D. and Parsons, J., 2005. Enhanced performance through multilayer coating. In: *Proceedings of TAPPI Coating conference and exhibit 2005*, Toronto, Canada, 17–20 April 2005. Atlanta: TAPPI Press.

James, G., Witten, D., Hastie, T. and Tibshirani, R., 2013. *An Introduction to Statistical Learning – with Applications in R*. [ebook] New York: Springer-Verlag.

Jensen, K.W., 1989. Flexo printability of coated white-top liner with consideration of convertability. *Graphic Arts in Finland*, 18(1), pp. 14–20.

Lagerstedt, P. and Kolseth, P., 1995. Influence of surface energetics on ink transfer in flexo printing. In: *Advances in Printing Science and Technology: Proceedings of the 23th International Research Conference of iarigai*. Paris, France, 17–20 September 1995. Chichester, UK: John Wiley & Sons, pp. 269–299.

Lucas, R., 1918. Ueber das Zeitgesetz des kapillaren Aufstiegs von Flüssigkeiten. *Kolloid-Zeitschrift*, 23(1), pp. 15–22.

Olsson, R., Yang, L., Van Stam, J. and Lestelius, M., 2006. Effects on ink setting in flexographic printing: coating polarity and dot gain. *Nordic Pulp & Paper Research Journal*, 21(5), pp. 569–574.

Owens, D.K. and Wendt, R.C., 1969. Estimation of the surface free energy of polymers. *Journal of Applied Polymer Science*, 13(8), pp. 1741–1747.

Preston, J., Hiorns, A., Parsons, D.J. and Heard, P., 2008. Design of coating structure for flexographic printing. *Paper Technology*, 49(3), pp. 27–36.

Ridgway, C.J. and Gane, P.A.C., 2002. Controlling the absorption dynamic of water-based ink into porous pigmented coating structures to enhance print performance. *Nordic Pulp & Paper Research Journal*, 17(2), pp. 119–129.

Sheng, Y.J., Shen, W. and Parker, I.H., 2000. Importance of the substrate surface energetics in water-based flexographic printing. *Appita Journal*, 53(5), pp. 367–370.

Thorman, S., Ström, G., Hagberg, A. and Johansson, P.-Å., 2012. Uniformity of liquid absorption by coatings – technique and impact of coating composition. *Nordic Pulp & Paper Research Journal*, 27(2), pp. 459–465.

Thorman, S., Yang, L. and Hagberg, A., 2013. Simultaneous determination of absorption mottle and white-top mottle in the same area on coated boards. In: N. Enlund and M. Lovreček, eds. *Advances in Printing and Media Technology: Proceedings of the 40th International Research Conference of iarigai*. Chemnitz, Germany, 8–11 September 2013. Darmstadt, Germany: iarigai, pp. 225–232.

Washburn, E.W., 1921. The Dynamics of Capillary Flow. *Physical Review*, 17(3), pp. 273–283.

Wågberg, P. and Wennerblom, A., 1992. A correlation between results achieved with an optical profile tester, conventional paper evaluation and printability. In: *Proceedings of TAPPI International Printing and Graphic Arts Conference*, Pittsburgh, USA, 18–21 October 1992. Atlanta: TAPPI Press, pp. 187–196.